Electronic Supplementary Information

Computational elucidation of the binding mechanisms of curcumin analogues as bacterial RecA inhibitors

Zi-Yuan Zhou,[†,§,#] Jing Yuan,[†,#] Qing Pan,[‡] Xiao-Mei Mo,[†] Yong-Li Xie,[†] Feng Yin,[§] Zigang Li,[*,§] Nai-Kei Wong[*,†]

[†]Department of Infectious Diseases, Shenzhen Third People's Hospital, The Second Hospital Affiliated to Southern University of Science and Technology, Shenzhen 518112, China

[§]Department of Chemical Biology, School of Chemical Biology and Biotechnology, Shenzhen Graduate School of Peking University, Shenzhen 518055, China.

[‡]Shenzhen Key Laboratory of Microbial Genetic Engineering, College of Life Sciences and Oceanology, Shenzhen University, Shenzhen 518055, China

Table of Contents

1. Potential antibacterial agents: from turmeric to curcumin analogues

Curcumin has shown potential of an antibacterial agent.[1-2] For example, the antimicrobial photodynamic therapy (PDT) is a treatment approach that utilizes reactive oxygen species (ROS) produced by non-toxic dye or photosensitizer (PS) molecules including curcumin in the presence of low intensity visible light to eradicate microbial pathogens.[1] As light is required for drug activation, it is believed that bacteria would not be able to develop resistance to PDT easily.[1-2]

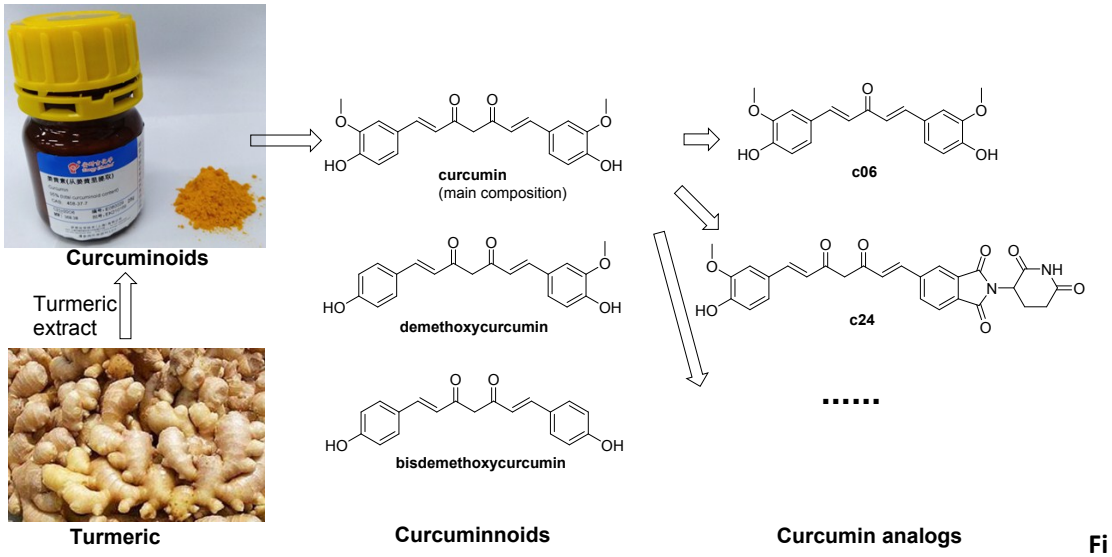

Figure S1. Sources and structural relations of turmeric and curcumin analogues. [2-4]

2. Prediction on the probability of residues forming a binding site

Depth is a web server for predicting small-molecule ligand-binding pockets and computing their depth and cavity sizes, detecting potential and predicting the pK_a of ionisable residues in proteins. Depth also uses water molecules as probes and measures the closest distance of a residue to bulk solvent (**Figure S2**, left).[5] By giving a cut-off value for the probability of residues forming a binding site, it can also predict the key residues that engage in important interactions within a target protein.[5] The Depth predicted binding residues (with minimum number of neighbourhood water of 4 and cavity prediction probability threshold of 0.98) are as follows: Thr39, Ile40, Ser41, Thr42, Gly43, Leu45, Asp48, 54, Glu68, Lys72, Gln78, Val79, Gln84, Arg85, Glu86, Lys88, Gly96, Tyr103, Asp144, Phe270, Tyr271, Lys317, Glu320, Arg324, Ser333. Results for some of these residues are consistent with the predictions made by eF-seek in **Figure 2** and SiteHound in **Figure 3**.

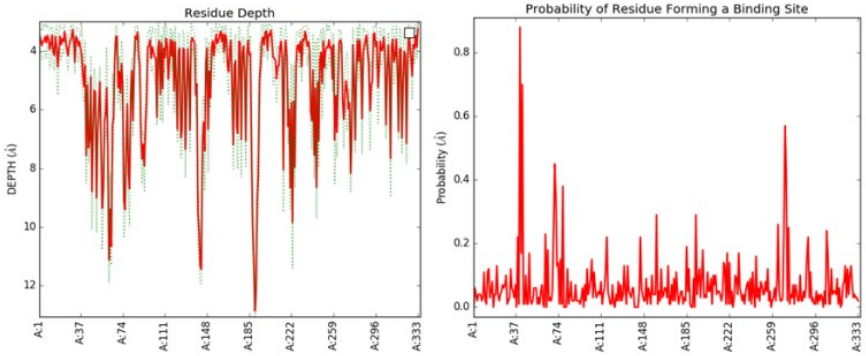

Figure S2. Probability of residues forming a binding site and residue depth plot. The above pots are generated by Depth[5].

3. Binding pocket prediction by GHECOM

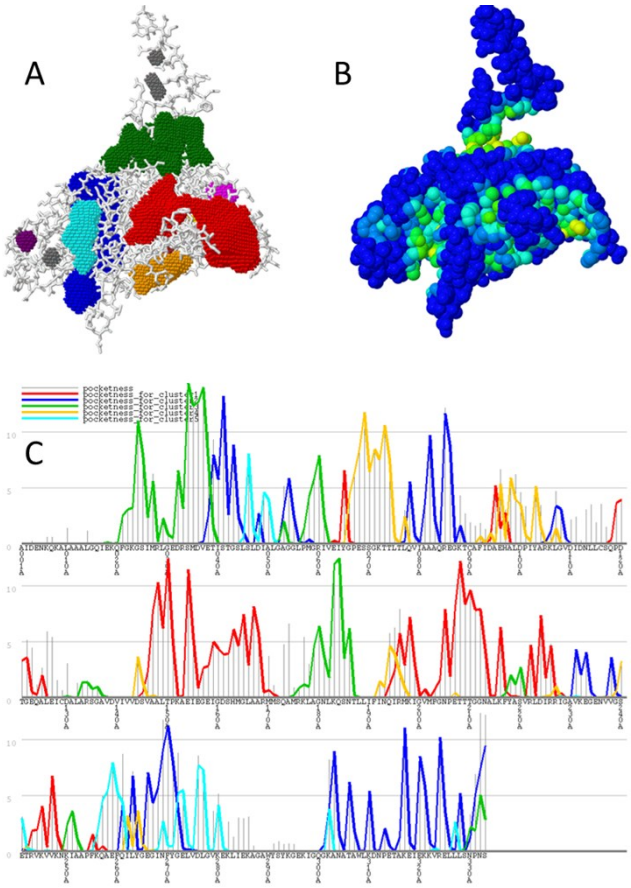

Figure S3. GHECOM[6-7] results showing (A) Jmol view of pocket structures and their locations, red: pocket D (ssDNA binding region); blue: pocket B; orange: pocket A (ATPase activity region); cyan: pocket C (dsDNA interaction region). (B) Jmol view of pocket structure based on 'pocketness' (the term 'pocketness' was introduced by Takeshi Kawabata et al. to indicate both the size and depth of a pocket)[6]. The proportion of $R_{inaccess}$ values (The term '$R_{inaccess}$' was used by Takeshi Kawabata et al. to indicate the inaccessibility of each residue)[7] for ligand atoms. Each colour corresponds to a specific $R_{inaccess}$ value of the probe dummy atoms. The red, orange, yellow, green, cyan, blue, and deep blue 'pocketness' colours correspond to 2–3 Å, 3–4 Å, 4–5 Å, 5–6 Å, 6–7 Å, 7–10 Å, and >10 Å, respectively. (C) Jmol view of graph residue-based pocketness [percentage %] for each residue (red: cluster 1, blue: cluster 2, green: cluster 3, orange: cluster 4, cyan: cluster 5. These colours correspond to the colours in **Figure S3A**). The GHECOM server discovers 5 pockets on RecA surfaces using mathematical morphology (**Figure S3**). These results resemble the GHECOM results generated through metaPocket 2.0 web server, but are not identical. This disparity could be a result of different default parameters used. The predictions are largely consistent with the pocket and residue predictions discussed in **Figures 1** and **3**.

4. Grid box parameters of docking studies

Table S1. Grid box parameters applied in Autodock Vina calculations in this study.

Pocket	Center coordinates[a] (x, y, z)	Box sizes[a] (x, y, z)
A	(42.0, 19.0, 5.0)	(20.0, 20.0, 24.0)
B	(55.0, 24.0, -17.0)	(32.0, 24.0, 24.0)
C	(53.0, 45.0, -5.0)	(30.0, 22.0, 22.0)
D	(56.0, 18.0, 23.0)	(24.0, 26.0, 24.0)

[a] Coordinate values or size values are all in Å

Table S2. Grid box parameters applied in Ledock calculations in this study.

Pocket	box boundaries[b]		
	x	**y**	**z**
A	(32.0, 52.0)	(9.0, 29.0)	(-7.0, 19.0)
B	(39.0, 71.0)	(12.0, 36.0)	(-39.0, -5.0)
C	(38.0, 68.0)	(34.0, 56.0)	(-16.0, 6.0)
D	(44.0, 68.0)	(5.0, 31.0	(11.0, 35.0)

[b] Coordinate values or size values are all in Å

5. DFT calculations

The Gaussian computational results were obtained with level of theory in the main article. The corresponding energy profiles are plotted in **Figure 4** of the main article.

Cartesian coordinates:

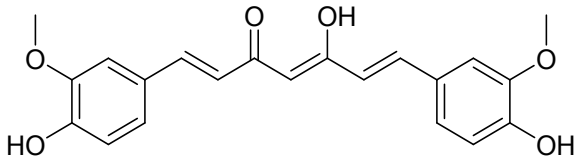

Curcumin tautomer 1 (enol form)

C	7.428717	-0.099586	-0.000272
C	7.610527	1.301383	0.001715
C	6.499487	2.143902	0.003354
C	5.215036	1.607467	0.002998
C	5.012878	0.215025	0.001025
C	6.147035	-0.631345	-0.000553
C	3.694141	-0.403669	0.000548
C	2.485536	0.203809	0.000826
C	1.235374	-0.567675	0.000321
C	-0.003114	0.163079	0.000076
O	1.252372	-1.837578	0.000095
C	-1.223257	-0.492237	-0.000370
C	-2.482466	0.223551	-0.000697
O	-1.284917	-1.828026	-0.000512
C	-3.686362	-0.398292	-0.000723
C	-5.005364	0.219300	-0.001147
C	-5.210547	1.611493	-0.003117
C	-6.496113	2.145180	-0.003386
C	-7.605646	1.300804	-0.001670
C	-7.420887	-0.099802	0.000281
C	-6.138279	-0.629113	0.000473
O	8.601829	-0.803145	-0.001738
C	8.539065	-2.229251	-0.004761
O	8.864571	1.824111	0.002033
O	-8.860677	1.821189	-0.001900
O	-8.592437	-0.805749	0.001781
C	-8.526943	-2.231755	0.005174
H	6.658867	3.217722	0.004888
H	4.365351	2.282364	0.004345
H	6.001131	-1.706112	-0.002040
H	3.684043	-1.492979	-0.000191
H	2.390036	1.286350	0.001331

H	0.011146	1.246543	0.000222
H	-2.402429	1.306657	-0.000828
H	-3.681240	-1.486574	-0.000286
H	-4.363323	2.289422	-0.004568
H	-6.657272	3.218725	-0.004918
H	-5.990828	-1.703659	0.001931
H	8.027703	-2.601233	0.890353
H	9.573535	-2.573575	-0.005991
H	8.026825	-2.597367	-0.900973
H	9.490299	1.075757	0.000573
H	-9.485056	1.071717	-0.000353
H	-9.560758	-2.578020	0.006605
H	-8.014992	-2.602956	-0.889920
H	-8.013917	-2.598611	0.901443
H	-0.317963	-2.134188	-0.000283

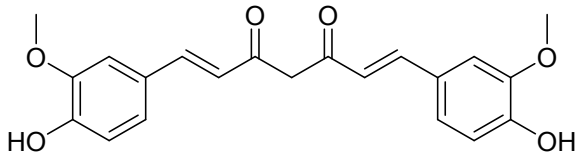

Curcumin tautomer 2 (keto form)

C	-5.474802	-1.285667	0.445358
C	-5.052109	-2.255830	-0.491751
C	-3.937229	-2.008765	-1.292879
C	-3.241970	-0.810144	-1.170684
C	-3.647121	0.168626	-0.243764
C	-4.780056	-0.091237	0.564580
C	-2.959598	1.437645	-0.071902
C	-1.855492	1.889992	-0.713853
C	-1.295097	3.214427	-0.407788
C	-0.012510	3.612533	-1.153214
O	-1.783712	3.982418	0.419104
C	1.214733	3.180162	-0.334965
C	1.842772	1.902278	-0.699285
O	1.606131	3.888254	0.591542
C	2.909708	1.430634	-0.009532
C	3.652219	0.200721	-0.228587
C	3.338214	-0.718945	-1.247047

C	4.082382	-1.882275	-1.412957
C	5.156640	-2.152007	-0.565072
C	5.487651	-1.241448	0.464302
C	4.743700	-0.082440	0.627794
O	-6.577885	-1.661672	1.159971
C	-7.091512	-0.760785	2.141443
O	-5.731416	-3.424199	-0.610787
O	5.884060	-3.285710	-0.725988
O	6.559708	-1.635282	1.215549
C	6.988675	-0.790786	2.283950
H	-3.629350	-2.766426	-2.006603
H	-2.378606	-0.637624	-1.804579
H	-5.097962	0.658070	1.281348
H	-3.388845	2.110268	0.670258
H	-1.352161	1.297312	-1.472119
H	0.008830	3.165497	-2.151356
H	0.003814	4.701637	-1.232036
H	1.423367	1.361397	-1.542346
H	3.257935	2.052294	0.814933
H	2.506607	-0.528228	-1.917097
H	3.844430	-2.594491	-2.196751
H	4.991033	0.620706	1.415747
H	-6.346079	-0.563920	2.920253
H	-7.957116	-1.258439	2.579202
H	-7.402594	0.183982	1.681432
H	-6.468120	-3.398771	0.028464
H	6.580692	-3.283308	-0.042818
H	7.845340	-1.292094	2.734916
H	7.292518	0.192727	1.907989
H	6.195990	-0.671203	3.031157

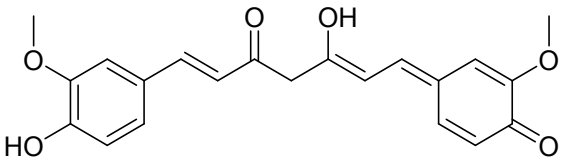

Curcumin tautomer 3 (quinone methide form)

C	-7.409708	-0.142086	-0.001328
C	-7.609702	1.258378	0.000126
C	-6.511481	2.119879	0.001830

C	-5.221288	1.603262	0.002076
C	-5.001077	0.211825	0.000655
C	-6.122174	-0.654663	-0.000992
C	-3.679859	-0.383077	0.000850
C	-2.475638	0.245819	0.001195
C	-1.233875	-0.512619	0.001576
C	0.050230	0.309542	0.001949
O	-1.203232	-1.757772	0.001697
C	1.371406	-0.438246	0.001516
C	2.560155	0.251354	0.000898
O	1.354325	-1.770912	0.001900
C	3.822079	-0.389628	0.000606
C	5.081619	0.197841	-0.000260
C	5.288044	1.622922	-0.001197
C	6.540003	2.156460	-0.001892
C	7.744504	1.335236	-0.001623
C	7.516633	-0.125938	-0.000826
C	6.254741	-0.645997	-0.000121
O	-8.572869	-0.857865	-0.003022
C	-8.494242	-2.284161	-0.003291
O	-8.866836	1.761525	-0.000100
O	8.889909	1.822892	-0.002033
O	8.673884	-0.845058	-0.000888
C	8.567245	-2.264218	0.000838
H	-6.688483	3.190624	0.003011
H	-4.381241	2.289693	0.003531
H	-5.959275	-1.726769	-0.002050
H	-3.652724	-1.471997	0.000652
H	-2.392384	1.328589	0.001179
H	0.018105	0.980954	0.871023
H	2.492508	1.334282	0.000655
H	3.797286	-1.478033	0.001213
H	4.426328	2.283916	-0.001403
H	6.694865	3.232002	-0.002596
H	6.096832	-1.719791	0.000517
H	-7.977989	-2.647029	-0.899117
H	-9.524887	-2.639197	-0.003911
H	-7.978905	-2.647415	0.892905
H	-9.484912	1.006154	-0.001147
H	9.590187	-2.643975	0.001197
H	8.042834	-2.623898	0.895222
H	8.042682	-2.626111	-0.892569
H	0.393960	-2.057807	0.002016
H	0.018068	0.982036	-0.866265

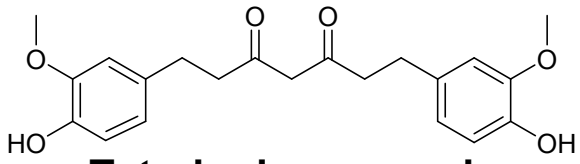

Tetrahydrocurcumin (keto form)

C	6.648334	-0.588178	0.322961
C	6.829697	-1.194734	-0.938110
C	5.979057	-0.864299	-1.985639
C	4.949432	0.063372	-1.785531
C	4.757151	0.670907	-0.542549
C	5.623606	0.334021	0.514629
C	3.623921	1.649633	-0.313494
C	2.377627	0.981061	0.285936
C	1.229300	1.935556	0.544752
C	-0.071514	1.325435	1.058676
O	1.314878	3.137476	0.353964
C	-0.929992	0.739385	-0.068019
C	-2.334145	0.316861	0.324612
O	-0.502431	0.623583	-1.204719
C	-3.119368	-0.364912	-0.807655
C	-4.517730	-0.763854	-0.383557
C	-4.787269	-2.045069	0.103468
C	-6.074063	-2.402795	0.523483
C	-7.108184	-1.477154	0.459157
C	-6.851139	-0.179727	-0.032561
C	-5.569681	0.169325	-0.448921
O	7.557878	-0.995939	1.264739
C	7.456099	-0.461213	2.582462
O	7.841020	-2.096517	-1.123964
O	-8.369681	-1.817638	0.862479
O	-7.957615	0.629796	-0.050227
C	-7.813028	1.966978	-0.523707
H	6.131603	-1.333343	-2.953326
H	4.293089	0.314828	-2.614883
H	5.489028	0.804574	1.483436
H	3.347262	2.127429	-1.259950
H	2.004065	0.184008	-0.371036
H	0.127595	0.519365	1.777461
H	-0.647352	2.095698	1.583362
H	-2.263264	-0.340472	1.202402

H	-2.564504	-1.249093	-1.140265
H	-3.988400	-2.780577	0.155309
H	-6.285239	-3.400241	0.897829
H	-5.374607	1.165684	-0.832664
H	7.587408	0.627163	2.578158
H	8.259651	-0.923735	3.156736
H	6.489451	-0.710886	3.035330
H	8.309086	-2.177405	-0.273068
H	-8.931731	-1.032728	0.729303
H	-8.801206	2.421537	-0.444555
H	-7.099838	2.527902	0.091525
H	-7.484608	1.981885	-1.569504
H	2.620552	0.485394	1.237517
H	3.948223	2.454288	0.356403
H	-3.163426	0.316191	-1.664917
H	-2.863897	1.212846	0.678869

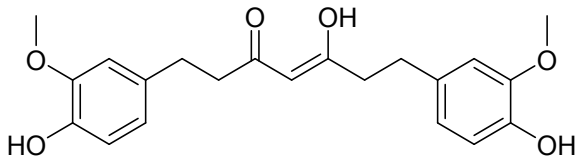

Tetrahydrocurcumin (enol form)

C	6.456862	1.098592	0.265499
C	7.187342	0.793593	-0.902492
C	6.801493	-0.284620	-1.689262
C	5.693528	-1.058439	-1.322722
C	4.959109	-0.766720	-0.170825
C	5.356698	0.324968	0.623945
C	3.738700	-1.579049	0.210652
C	2.432268	-0.947586	-0.295671
C	1.178210	-1.717786	0.080116
C	-0.097840	-1.175789	-0.322768
O	1.266233	-2.792168	0.721739
C	-1.270229	-1.819015	-0.015627
C	-2.631916	-1.307037	-0.382872
O	-1.288426	-2.967392	0.663142
C	-3.490947	-0.961617	0.862583
C	-4.871668	-0.465691	0.489623

C	-5.947524	-1.349066	0.371626
C	-7.216259	-0.894803	-0.006737
C	-7.420910	0.453934	-0.271493
C	-6.343662	1.357807	-0.154764
C	-5.084342	0.899619	0.221777
O	6.945718	2.178954	0.954441
C	6.278275	2.579283	2.149058
O	8.270225	1.553365	-1.250068
O	-8.657472	0.907911	-0.637293
O	-6.683040	2.655965	-0.436296
C	-5.670075	3.655920	-0.352180
H	7.374930	-0.513496	-2.582866
H	5.405389	-1.901032	-1.946432
H	4.798795	0.557436	1.525502
H	3.681248	-1.684564	1.300124
H	2.327976	0.078517	0.083948
H	-0.133165	-0.244460	-0.875426
H	-2.529875	-0.425982	-1.023104
H	-2.963902	-0.201016	1.451103
H	-5.802113	-2.406177	0.579512
H	-8.054737	-1.579563	-0.094152
H	-4.256876	1.595600	0.316021
H	5.238501	2.860101	1.944470
H	6.824906	3.446179	2.521986
H	6.299977	1.780397	2.899451
H	8.360590	2.246247	-0.570836
H	-8.579298	1.870242	-0.769843
H	-6.155026	4.596860	-0.614471
H	-5.265146	3.722070	0.664379
H	-4.855963	3.452710	-1.057634
H	-0.324065	-3.183624	0.856244
H	-3.570415	-1.855425	1.489973
H	-3.148973	-2.081891	-0.963497
H	2.454549	-0.848050	-1.390243
H	3.824108	-2.593130	-0.194325

6. Binding mechanism studies on curcumin building blocks and additional curcumin analogous as RecA specific inhibitors

To investigate whether the curcumin-thalidomide hybrids are more potent than other curcumin like compounds, two more groups of curcumin like compounds were added, followed by computational investigations. **Scheme S1** depicts some reported "building blocks" of curcumin, including coniferyl aldehyde (**c43**), *p*-coumaric acid (**c45**), caffeic acid (**c46**), ferulic acid (**c47**), sinapic acid (**c48**), sinapaldehyde (**c50**), coniferyl alcohol (**c51**), sinapyl alcohol (**c52**), resveratrol (**c53**), hydroxytyrosol (**c54**), etc. **Scheme S2** shows reported curcumin-like compounds.[8] **c61**-**c64** are compounds which have shown senolytic activities.[9] **c65**-**c85** are curcumin-like compounds designed and synthesized with the aims of blocking bacterial sialidase.[10]

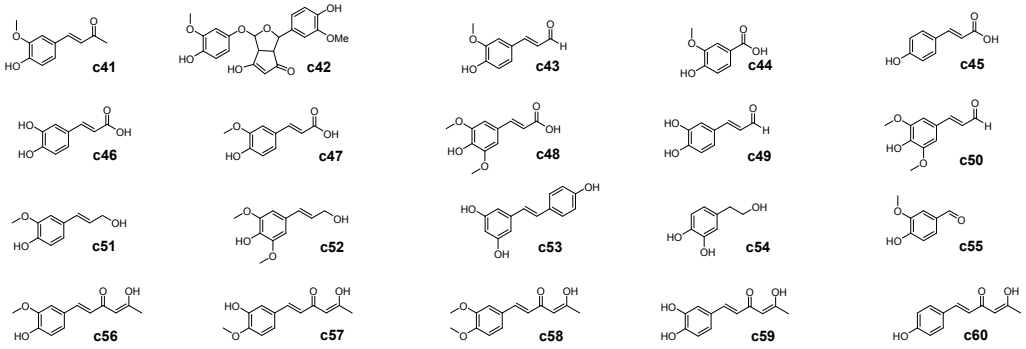

Scheme S1. Molecular structures of reported curcumin building blocks.[8]

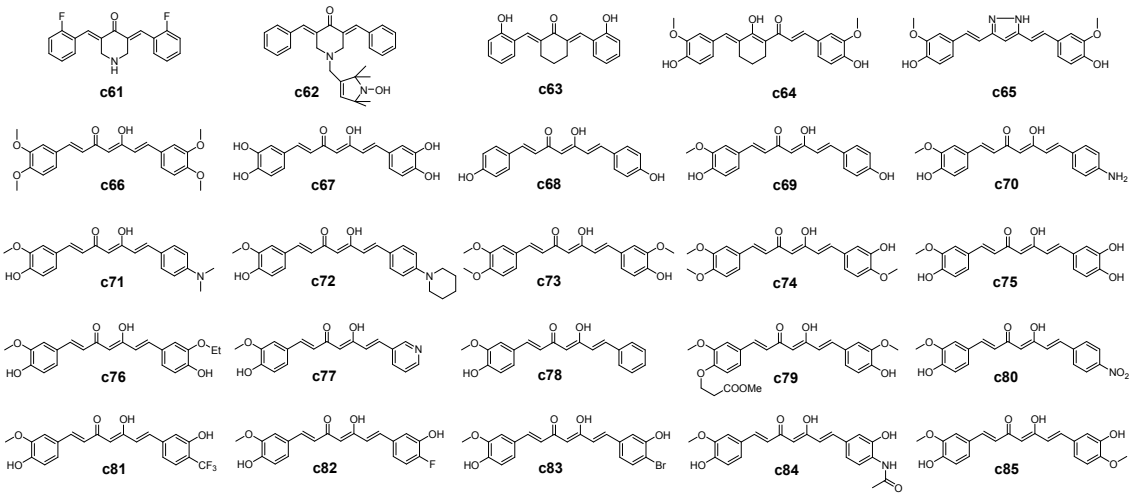

Scheme S2. Molecular structures of additional curcumin analogous reported

Table S3. Estimated binding energies for the binding between curcumin-thalidomide analogues and *E. coli* RecA protein.

Entry	Estimated binding energies (kcal/mol)*			
	Pocket A	**Pocket B**	**Pocket C**	**Pocket D**
c41	-5.5 (-2.52)	-5.9 (-2.42)	5.4- (-2.33)	-4.4 (-2.48)
c42	-7.8 (-3.36)	-8.6 (-2.76)	-7.9 (-2.67)	-7.0 (-3.40)
c43	-5.2 (-2.42)	-5.9 (-2.24)	-5.3 (-2.38)	-4.4 (-2.48)
c44	-5.1 (-1.66)	-5.5 (-1.50)	-5.2 (-1.61)	-4.5 (-1.44)
c45	-5.4 (-1.77)	-6.0 (-1.74)	-5.3 (-1.78)	-4.6 (-1.76)
c46	-5.4 (-2.52)	-6.1 (-2.44)	-5.4 (-2.04)	-4.8 (-2.32)
c47	-5.7 (-1.81)	-6.1 (-1.84)	-5.6 (-1.65)	-4.5 (-1.86)
c48	-5.7 (-1.67)	-6.3 (-1.08)	-5.6 (-1.93)	-4.5 (-1.73)
c49	-5.2 (-2.57)	-5.9 (-2.51)	-5.2 (-2.37)	-4.3 (-2.48)
c50	-5.4 (-2.38)	-5.9 (-2.76)	-5.2 (-2.53)	-4.3 (-2.34)
c51	-5.2 (-3.05)	-6.0 (-2.99)	-5.1 (-3.08)	-4.3 (-2.78)
c52	-5.3 (-3.20)	-5.9 (-2.89)	-5.3 (-2.97)	-4.3 (-2.98)
c53	-5.3 (-3.19)	-5.8 (-2.90)	-5.2 (-2.87)	-4.3 (-2.83)
c54	-5.0 (-3.31)	-5.5 (-3.05)	-4.6 (-3.27)	-4.8 (-3.11)
c55	-4.9 (-2.06)	-5.2 (-2.10)	-4.7 (-2.24)	-4.4 (-2.14)
c56	-6.4 (-2.62)	-6.7 (-2.64)	-5.9 (-2.42)	-5.0 (-2.24)
c57	-6.4 (-2.39)	-6.9 (-2.44)	-6.0 (-2.38)	-5.2 (-2.38)
c58	-6.2 (-2.08)	-6.7 (-1.92)	-5.9 (-1.98)	-5.1 (-1.90)
c59	-6.5 (-3.20)	-7.1 (-3.12)	-5.9 (-2.74)	-5.1 (-2.82)
c60	-6.0 (-2.57)	-6.7 (-2.39)	-5.9 (-2.36)	-5.1 (-2.26)
c61	-7.5 (-4.44)	-8.0 (-4.27)	-7.6 (-4.26)	-6.2 (-3.19)
c62	-9.1 (-4.87)	-8.3 (-4.74)	-7.4 (-4.21)	-6.8 (-4.39)
c63	-7.7 (-4.37)	-7.9 (-4.20)	-7.0 (-3.66)	-5.9 (-3.73)
c64	-9.2 (-4.27)	-8.8 (-4.07)	-7.5 (-3.32)	-6.4 (-3.83)
c65	-7.9 (-5.56)	-8.0 (-4.73)	-7.2 (-4.75)	-5.7 (-4.65)
c66	-7.3 (-3.08)	-8.2 (-2.63)	-6.4 (-2.34)	-5.8 (-2.68)
c67	-7.9 (-4.65)	-9.3 (-4.94)	-6.8 (-4.61)	-6.4 (-4.11)
c68	-7.3 (-3.82)	-8.3 (-3.47)	-7.0 (-3.70)	-5.8 (-3.31)
c69	-7.4 (-4.19)	-8.5 (-4.11)	-6.6 (-3.53)	-5.8 (-3.10)
c70	-7.5 (-4.50)	-8.5 (-4.72)	-6.6 (-4.51)	-5.9 (-4.00)
c71	-7.7 (-3.83)	-8.0 (-3.91)	-6.6 (-3.05)	-5.9 (-3.38)
c72	-8.0 (-4.25)	-8.8 (-4.16)	-6.9 (-3.28)	-6.7 (-3.28)
c73	-7.3 (-3.55)	-8.6 (-3.36)	-6.4 (-3.06)	-5.8 (-3.09)
c74	-7.7 (-3.86)	-8.3 (-3.22)	-6.5 (-2.95)	-5.9 (-3.33)
c75	-8.0 (-4.16)	-8.9 (-4.16)	-7.0 (-4.01)	-6.2 (-3.93)
c76	-7.6 (-3.93)	-8.3 (-3.50)	-6.2 (-3.26)	-5.9 (-3.31)
c77	-7.7 (-4.03)	-8.0 (-3.98)	-6.8 (-3.95)	-5.7 (-3.44)
c78	-7.7 (-3.44)	-8.1 (-3.13)	-6.9 (-3.01)	-5.9 (-2.97)
c79	-7.4 (-3.27)	-8.4 (-3.85)	-6.6 (-3.23)	-5.8 (-3.46)
c80	-7.3 (-3.62)	-8.4 (-4.06)	-6.5 (-3.61)	-5.6 (-3.10)

c81	-8.1 (-4.30)	-8.9 (-3.60)	-7.0 (-3.41)	-6.4 (-3.58)
c82	-8.1 (-4.24)	-8.8 (-3.41)	-6.7 (-3.79)	-6.0 (-3.71)
c83	-8.0 (-4.66)	-8.6 (-3.80)	-6.6 (-3.77)	-6.0 (-3.90)
c84	-8.3 (-5.44)	-8.1 (-4.13)	-6.9 (-4.38)	-6.2 (-4.62)
c85	-7.9 (-3.94)	-8.7 (-3.53)	-6.5 (-3.63)	-6.0 (-3.52)

***** Binding energies outside the brackets were estimated by Autodock Vina and binding energies within the brackets were estimated by Ledock (http://www.lephar.com/)

The additional curcumin analogues in **Scheme S2** are predicted to be more potent inhibitors than the building blocks in the **Scheme S1**. Compared with the curcumin-thalidomide hybrids in the **scheme 2**, no significantly higher binding scores were observed for the compounds in **Scheme S1** or **Scheme S2**. This applies to both of the binding energies generated by Autodock Vina and Ledock. In addition, the estimated binding energies obtained with Autodock Vina and Ledock agree with each other, with R = 0.781 (**Figure S4**). The compound **c64**, which is predicted to be one of the most potent inhibitor in **Scheme S1** and **Scheme S2**, was further analyzed for its binding energy by MM-GBSA (**Table 2**), though the ΔG_{bind} of **c64** showed no significant difference compared with curcumin.

7. Details of the MM-GBSA calculation

The force field-based method MM-GBSA calculates the free energies of binding (ΔG_{bind})[11-12] from the change between the bound complex (ΔG_{cpx}) and unbound receptor (ΔG_{rec}) and unbound ligand in solution (ΔG_{lig}).[13-14]

$$\Delta G_{bind} = \Delta G_{cpx} - (\Delta G_{rec} + \Delta G_{lig}) \quad (1)$$

Each of ΔG_{cpx}, ΔG_{rec}, ΔG_{lig} could be further resolved into gas-phase molecular mechanics energy (ΔG_{MM}), polar and nonpolar solvation terms (ΔG_{solv}) , and an entropy terms (ΔS) at a predefined temperature (T). Took the ΔG_{cpx} for example:

$$\Delta G_{cpx} = \Delta G_{MM(cpx)} + \Delta G_{solv(cpx)} - T \cdot \Delta S_{cpx} \quad (2)$$

$$\Delta G_{rec} = \Delta G_{MM(rec)} + \Delta G_{solv(rec)} - T \cdot \Delta S_{rec} \quad (3)$$

$$\Delta G_{lig} = \Delta G_{MM(lig)} + \Delta G_{solv(lig)} - T \cdot \Delta S_{lig} \quad (4)$$

In the above equation, ΔE_{MM} could be calculated by the sum of chemical bonds, angles, and torsion terms ΔE_{bat}, which are defined by force field, plus the van der Waals ΔG_{vdW} and Coulombic terms ΔE_{coul}. The solvation term could be further resolved into a polar contribution, and nonpolar contribution. The contributions of the polar contributions are calculated by a Poisson-Boltzamn (PB) distribution in MM-PBSA and generalized-Born (GB) approximations in MM-GBSA[12, 15], whereas the nonpolar contribution is usually estimated as a linear function of the solvent accessible surface area[15]. Consider the case of the ΔG_{cpx}, for example.

$$\Delta G_{cpx} = \Delta E_{bat(cpx)} + \Delta G_{vdW(cpx)} + \Delta E_{coul(cpx)} + \Delta G_{solv,p(cpx)} + \Delta G_{solv,np(cpx)} - T \cdot \Delta S \quad (5)$$

Although some of the computational scientists still advocate the calculation and inclusion of the entropy in the binding energy estimation,[16] it apparently presents some disadvantages for the calculation of entropy is usually time consuming and could itself be a major source of error[13, 17]. For this reason, the entropy term is neglected in our computation[17]. Combining (1) to (5), ΔG_{bind} could be calculated:

$$\Delta G_{bind} = [\Delta G_{MM(cpx)} - (\Delta G_{MM(rec)} + \Delta G_{MM(lig)})] + [\Delta G_{solv(cpx)} - (\Delta G_{solv(rec)} + \Delta G_{solv(lig)})] = \Delta G_{MM} + \Delta G_{solv} \quad (6)$$

8. Correlation of binding energies predicted by two docking algorithms in this study

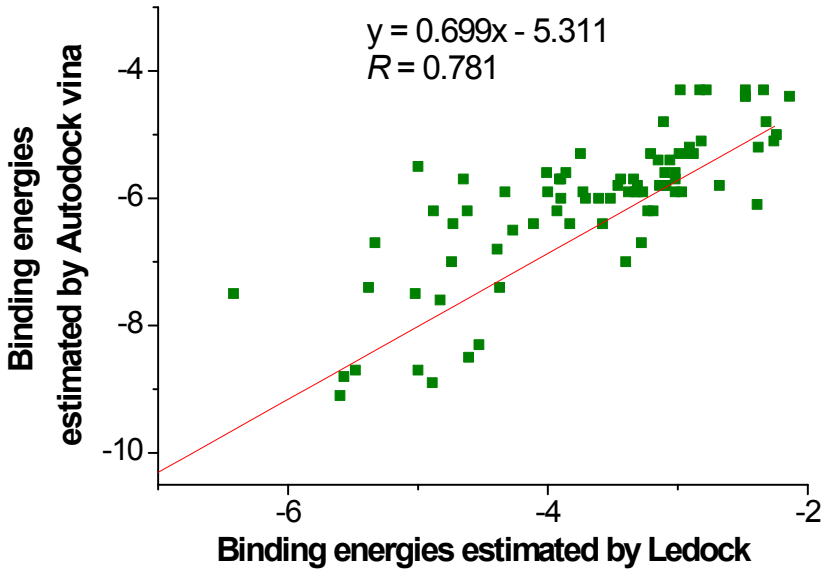

Figure S4. Correlation of binding energies (kcal/mol) between compounds **c01**-**c85** and RecA protein (pocket D) predicted by AutoDock Vina and Ledock.

References

1 Soria-Lozano, P.; Gilaberte, Y.; Paz-Cristobal, M. P.; Perez-Artiaga, L.; Lampaya-Perez, V.; Aporta, J.; Perez-Laguna, V.; Garcia-Luque, I.; Revillo, M. J.; Rezusta, A., *BMC Microbiol.* 2015, **15**, 187/1-187/8.

2 Nelson, K. M.; Dahlin, J. L.; Bisson, J.; Graham, J.; Pauli, G. F.; Walters, M. A., *J. Med. Chem.* 2017, **60**, 1620-1637.

3 Priyadarsini, K. I., *Molecules* 2014, **19**, 20091-20112.

4 Niranjan, A.; Singh, S.; Dhiman, M.; Tewari, S. K., *Accessions. Anal. Lett.* 2013, **46**, 1069-1083.

5 Tan, K. P.; Nguyen, T. B.; Patel, S.; Varadarajan, R.; Madhusudhan, M. S., *Nucleic Acids Res.* 2013, **41**, 314-321.

6 Kawabata, T., *Proteins* 2009, **78**, 1195-1211.

7 Kawabata, T.; Go, N., *Proteins* 2007, **68**, 516-529.

8 Dogra, N.; Choudhary, R.; Kohli, P.; Haddock, J. D.; Makwana, S.; Horev, B.; Vinokur, Y.; Droby, S.; Rodov, V., *J. Agric. Food Chem.* 2015, **63**, 2557-2565.

9 Li, W.; Zhang, R.; Li, W.; He, Y.; Zhou, D.; Li, W.; Zheng, G., *Aging* 2019, **11**, 771-782.

10 Kim, B. R.; Park, J.-Y.; Jeong, H. J.; Kwon, H.-J.; Park, S.-J.; Lee, I.-C.; Ryu, Y. B.; Lee, W. S., *J. Enzyme Inhib. Med. Chem.* 2018, **33**, 1256-1265.

11 Massova, I.; Kollman, P. A., *Perspect. Drug Discov. Des.* 2000, **18**, 113-135.

12 Kollman, P. A.; Massova, I.; Reyes, C.; Kuhn, B.; Huo, S.; Chong, L.; Lee, M.; Lee, T.; Duan, Y.; Wang, W.; Donini, O.; Cieplak, P.; Srinivasan, J.; Case, D. A.; Cheatham, T. E., III, *Acc. Chem. Res.* 2000, **33**, 889-897.

13 Rastelli, G.; Del Rio, A.; Degliesposti, G.; Sgobba, M., *J. Comput. Chem.* 2010, **31**, 797-810.

14 Guimaraes, C. R. W.; Cardozo, *J. Chem. Inf. Model.* 2008, **48**, 958-970.

15 Greenidge, P. A.; Kramer, C.; Mozziconacci, J.-C.; Wolf, R. M., *J. Chem. Inf. Model.* 2013, 53, 201-209.

16 Lafont, V.; Armstrong, A. A.; Ohtaka, H.; Kiso, Y.; Amzel, L. M.; *Chem. Biol. Drug Des.* 2007, 69, 413-422.

17 Hou, T.-J.; Wang, J.-M.; Li, Y.-Y.; Wang, W., *J. Comput. Chem.* 2011, **32**, 866-877.